ELSEVIER

Journal of Nuclear Materials 307–311 (2002) 961–965

journal of nuclear materials

www.elsevier.com/locate/jnucmat

The effect of hydrogen and helium on microvoid formation in iron and nickel

T. Ishizaki [a,*], Q. Xu [a], T. Yoshiie [a], S. Nagata [b], T. Troev [c]

[a] *Research Reactor Institute, Kyoto University, Kumatori-cho, Sennan-Gun, Osaka 590-0494, Japan*
[b] *Institute for Materials Research, Tohoku University, 2-1-1 Katahira, Aoba-ku, Sendai 980-8577, Japan*
[c] *Bulgarian Academy of Sciences, 72 Tzarigradsko, Chaussee, Sofia 1784, Bulgaria*

Abstract

Irradiation experiments on iron and nickel were carried out to study the effect of hydrogen and helium ions on microvoid formation. The total dose was 1.0×10^{17} hydrogen ions/cm^2 (0.2 dpa) and 9.6×10^{15} helium ions/cm^2 (0.3 dpa). The irradiation temperature was 423 and 573 K. To investigate microvoid formation and the total amount of residual defects, positron annihilation lifetime and coincidence Doppler broadening measurements were made. The results for positron lifetime indicated that vacancy clusters grew more easily in nickel than in iron and helium atoms were more effective for microvoid formation than hydrogen atoms. The temperature dependence of microvoid growth was greater after irradiation with hydrogen ions than helium ions between 423 and 573 K in both metals. Annealing experiments for nickel irradiated with hydrogen and helium ions at 423 k were carried out at up to 573 K and the stability of helium–vacancy complexes was clarified.

1. Introduction

To develop materials for use in fusion reactors, it is necessary to study the influence of impurities generated by nuclear transmutation for the evolution of defective structures. Especially important are the effects of hydrogen and helium atoms on microvoid formation. As the rate of production of hydrogen and helium atoms is much higher in the fusion environment than in the fission environment, these gas atoms promote cavity nucleation [1,2]. However, a thorough qualitative study of the role of gas atoms in microvoid formation in metals (e.g. the properties of hydrogen–vacancy and helium–vacancy complexes) has not been made to date. In this study, in order to investigate the effects of hydrogen and helium atoms on microvoid formation in metals qualitatively, irradiation experiments of hydrogen and helium ions on pure iron and nickel were carried out at 423 and 573 K. As post-irradiation experiments, positron annihilation lifetime and coincidence Doppler broadening (CDB) measurements were made. The positron annihilation technique is effective for investigating microvoid formation because it can detect vacancy-type defects in solids [3,4]. Particularly, the CDB measurement by using two detectors, which determine the longitudinal momentum distribution of electrons annihilated with positrons, is a remarkable technique for detecting total induced defects and identifying the elements in and around a vacancy cluster [5–8]. This method has a great advantage for counting γ-rays because of a reduction in the disturbance from background spectra on the higher energy side of the annihilation peak (511 keV) [9]. The temperature-dependence of microvoid formation caused by hydrogen and helium ions was discussed based on the results of positron annihilation measurements. In addition, in order to investigate the stability of hydrogen–vacancy and helium–vacancy complexes in nickel, isochronal annealing experiments for nickel irradiated with hydrogen and helium ions at 423 K were performed and the change of positron lifetimes was investigated.

* Corresponding author.
E-mail address: ishizaki@post3.rri.kyoto-u.ac.jp (T. Ishizaki).

0022-3115/02/$ - see front matter
PII: S0022-3115(02)01279-5

2. Experiment

Pure iron (99.99%) and nickel (99.99%) specimens were used for the irradiation experiments. As starting materials, high-purity nickel and iron supplied by Johnson & Matthey Chemicals Ltd., were employed. Nickel specimens were annealed in a high vacuum below 1.0×10^{-4} Pa at 1173 K and iron specimens were annealed in high-purity hydrogen gas at 873 K. The thickness of the nickel and iron specimens was about 0.4 and 0.15 mm, respectively. The irradiation experiments were carried out using an accelerator at the Institute for Materials Research, Tohoku University. The ion beam was circular with a diameter of 5 mm. The total dose was 1.0×10^{17} hydrogen ions/cm^2 and 9.6×10^{15} helium ions/cm^2. In order to align the damage and gas–atom range of both forms of irradiation, the acceleration energy of hydrogen and helium ions was 1.0 and 3.3 MeV, respectively. The damage and gas–atom distributions were calculated by the TRIM code with a displacement energy of 24 eV for nickel and iron. The depth of damage and gas–atom peak was about 6 μm from the surface of specimen and the effective gas-containing zones was about 1 μm in the vicinity of gas peak for both types of irradiation. The amounts of effective damage and gas-concentration were estimated as the average of the damage and gas–atom distribution in the region of a full-width at half maximum. In the case of hydrogen ion, the damage was about 0.2 dpa, the damage rate was 2.4×10^{-5} dpa/s, and the amount of hydrogen concentration was about 2 at.%. While in the case of helium ion, the damage was about 0.3 dpa, the damage rate was 1.8×10^{-6} dpa/s, and the amount of helium concentration was about 0.3 at.%. The irradiation temperature was 423 and 573 K.

In this study, a ^{22}Na source of positrons with 1.28 MeV γ-ray radiation was used for the positron annihilation experiments. The radioactivity of the source was about 30 μCi for lifetime measurements and about 20 μCi for CDB measurements. The system for positron annihilation lifetime measurements in this study was the conventional fast–fast circuit with two BaF_2 scintillators and the time resolution of this system was about 220 ps. The lifetimes were calculated from analyses of annihilation spectra by the positron resolution program. In order to measure the CDB spectra, two Ge detectors were located at an interval of 400 mm and the difference in energies of annihilation two γ-rays was counted. The longitudinal momentum of electrons annihilated with positrons was calculated by dividing the difference of two γ-rays by the light speed. The overall energy resolution of two Ge-detectors was 1.6 keV, which was defined by a full-width at half maximum of 661.6 keV γ-rays generated by the ^{137}Cs standard radiation source.

3. Results

3.1. Positron lifetime measurements

The results of positron annihilation lifetime measurements for iron and nickel irradiated with hydrogen and helium ions are shown in Figs. 1 and 2. As can be seen from these figures, the increase in long lifetime in iron and nickel is almost the same at 423 and 573 K after both hydrogen and helium-ion irradiation. But the long lifetime is a little larger in nickel than in iron at 573 K. In addition, the intensity of long lifetime does not decrease in iron as much with irradiation temperature increase as in nickel. This suggests that the density of vacancy clusters in iron did not change much in this temperature range compared with nickel. Another remarkable fea-

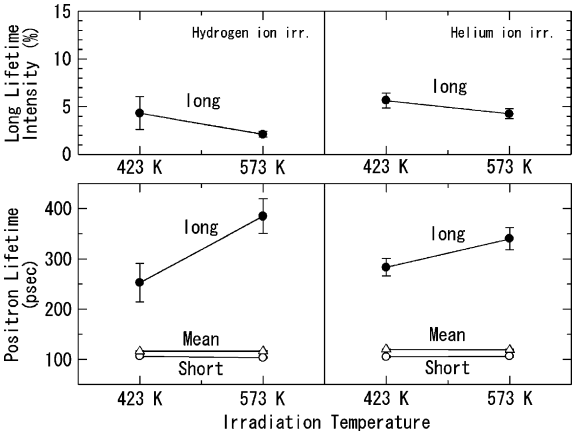

Fig. 1. Results of positron annihilation measurements for iron irradiated with hydrogen and helium ions at 423 and 573 K.

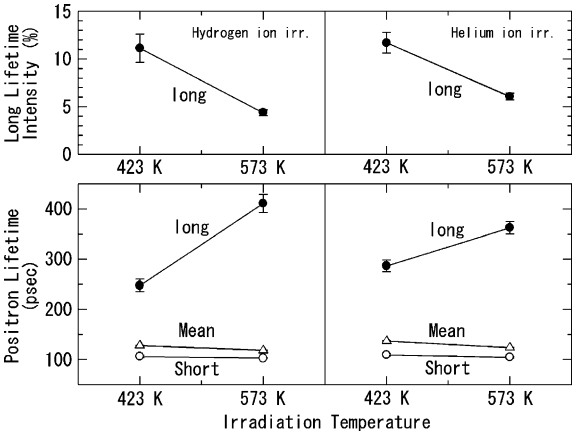

Fig. 2. Results of positron annihilation measurements for nickel irradiated with hydrogen and helium ions at 423 and 573 K.

ture of these results is that the increase in long lifetime is greater for hydrogen-ion irradiation than helium-ion irradiation between 423 and 573 K. In the case of hydrogen ion, the increase in long lifetime was 132.9 ps in iron and 163.4 ps in nickel. While, in the case of helium ion, it was 56.5 ps and 76.3 ps, respectively. This result indicates that the temperature dependence of microvoid growth was more prominent after irradiation with hydrogen ions rather than helium ions between 423 and 573 K.

3.2. Coincidence Doppler broadening measurements

Fig. 3 shows the CDB spectra of unirradiated nickel and nickel irradiated with hydrogen ions at 423 K (0.2 dpa). The mc of the x-axis unit gives the momentum, where m is the electron rest mass, c is the light speed and P_L is the longitudinal momentum of an electron annihilated with a positron. The unit of the y-axis is the count ratio for each momentum, which is normalized by dividing each count by the total count. A remarkable feature of this experiment is that the count ratio in the low momentum region of nickel irradiated with hydrogen ions is larger than that of unirradiated nickel. If positrons are trapped at open-volume defects such as vacancies, the count ratio in the low momentum region (for our experimental system, less than $5 \times 10^{-3}mc$ in the case of nickel) is larger than that of the unirradiated specimen because the electron momentum density of open-volume defects is concentrated in the low region. This low momentum region is called the S-region and the ratio of the S-region to the total count is called the S-parameter. The S-parameter is used as a measure of the total amount of vacancy-type defects. For example, if the S-parameter ratio between the unirradiated specimen and the specimen irradiated with high-energy particles is larger than 1.0, it can be considered that radiation-induced defects are formed.

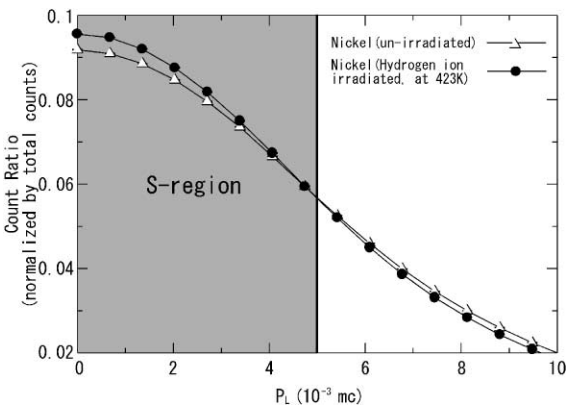

Fig. 3. Spectra from CBD measurements for unirradiated nickel and nickel irradiated with hydrogen ions at 423 K.

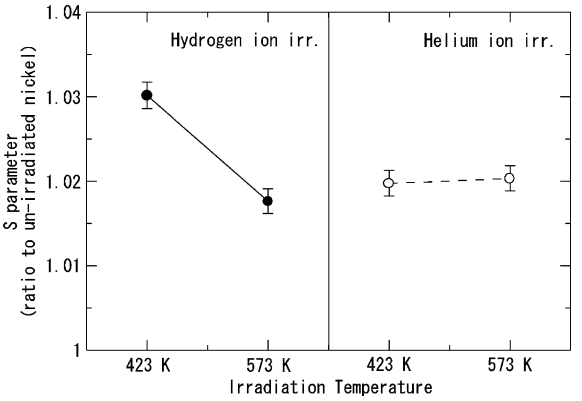

Fig. 4. S-parameter ratios between unirradiated nickel and nickel irradiated with hydrogen and helium ions at 423 and 573 K.

The S-parameter ratio of irradiated nickel to unirradiated nickel is plotted between 423 and 573 K in Fig. 4. The S-parameter ratio of nickel irradiated with hydrogen ions at 423 K is higher that that at 573 K. On the other hand, the S-parameter ratio of nickel irradiated with helium ions at 423 K is almost the same as that at 573 K.

3.3. Annealing experiments

In order to ascertain the stability of hydrogen–vacancy and helium–vacancy complexes in nickel, annealing experiments for nickel irradiated with hydrogen and helium ions at 423 K were carried out and the positron annihilation lifetimes after each annealing process were measured. The annealing time was 1 h and the annealing temperature was from 473 to 573 K. Fig. 5 shows the change of long lifetime components of nickel

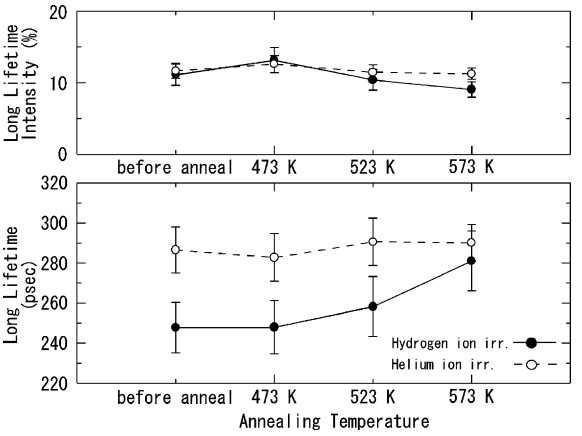

Fig. 5. Isochronal annealing behavior of long lifetime in nickel irradiated with hydrogen and helium ions at 423 K.

as a function of annealing temperature. From the annealing behavior of long lifetime components, it is clear that vacancy clustering occurred in nickel irradiated with hydrogen ions between 473 and 573 K but not in nickel irradiated with helium ions.

4. Discussion

The positron lifetime measurements indicated a difference and a similarity in microvoid formation between iron and nickel in this temperature range. For example, in Figs. 1 and 2, there was little difference in the change of long lifetime with temperature increase between iron and nickel for both hydrogen and helium-ion irradiation. A difference was only found in the intensity of long lifetime, i.e. the intensity of long lifetime was greater in nickel than in iron for all cases. Because the intensity of long lifetime corresponds to the density of vacancy clusters, the density of vacancy clusters was higher in nickel than in iron. This result reflects that the vacancy clustering is more efficient in nickel than in iron [10]. Despite the above difference in microvoid formation between nickel and iron, the basic behavior for microvoid formation was almost the same between hydrogen and helium-ion irradiation. The amount of damage was also similar between hydrogen (0.2 dpa) and helium (0.3 dpa) ion irradiation. But the amount of helium-atom concentration (0.3 at.%) was much smaller than that of hydrogen-atom concentration (2 at.%). Therefore the role of helium atoms in microvoid formation was more effective than that of hydrogen atoms.

The positron lifetime measurements also indicated that the temperature dependence of microvoid growth was greater for hydrogen-ion irradiation than helium-ion irradiation between 423 and 573 K. It was explained by the ease of dissociation of hydrogen–vacancy complexes. The migration activation energy of the hydrogen atom in iron is 0.059 eV [11] and the binding energy of the hydrogen–vacancy complex is 0.96 eV [12], while the migration activation energy of the hydrogen atom in nickel is 0.41 eV [13] and the binding energy of the hydrogen–vacancy complex is 0.57 eV [14]. The detrapping energy, a sum of the migration activation energy and the binding energy, of the hydrogen–vacancy complex in iron and nickel is about 1 eV. Therefore hydrogen atoms in iron and nickel easily escape from vacancies between 423 and 573 K. On the other hand, according to Reed, the detrapping energy of the helium–vacancy complex in iron is 3.9 eV and that in nickel is 3.2 eV [15]. So helium atoms in iron and nickel cannot escape from vacancies between 423 and 573 K.

The stability of hydrogen–vacancy and helium–vacancy complexes was also verified from the results of *S*-parameter ratios and annealing tests. In the case of hydrogen-ion irradiation, the *S*-parameter ratio was much higher at 423 K than at 573 K, i.e. the total amount of residual vacancies was much larger at 423 K. Because the de-trapping energy of the hydrogen–vacancy complex is about 1 eV, it can be considered that the complete decomposition of complexes occurs at 573 K. As some free vacancies were annihilated with sinks at 573 K, the total amount of residual vacancies decreased compared to the case at 423 K. On the other hand, the *S*-parameter ratio of nickel irradiated with helium ions at 423 K was almost the same as that at 573 K. The main reason for this result is the stability of helium–vacancy complexes in specimens. The open-volume defects were filled by helium atoms and the *S*-parameter ratio was apparently almost constant between 423 and 573 K.

The annealing behavior of nickel irradiated with hydrogen and helium ions at 423 K also revealed the stability of helium–vacancy complexes. According to Tanabe et al., in the case of deuterium ions implanted in nickel above 403 K, the thermal desorption spectrum of deuterium atoms has a single peak between 500 and 600 K [16]. Therefore it is considered that there existed some vacancies trapped by hydrogen atoms in the nickel specimen irradiated with hydrogen ions at 423 K. After annealing at high temperature, vacancy–hydrogen complexes decomposed into vacancies and hydrogen atoms. Therefore some free vacancies migrated and combined with vacancy clusters. Hence the growth of vacancy clusters occurred and the long lifetime increased as shown in Fig. 5. On the other hand, helium–vacancy complexes are very stable between 423 and 573 K. According to Yamauchi et al., in the case of helium ions implanted in nickel at room temperature, the thermal release of helium atoms in bubbles occurs around 1173 K [17] and helium atoms cannot escape from vacancies under 573 K. Therefore vacancies trapped by helium atoms could not migrate at all during the annealing and the growth of vacancy clusters did not occur.

5. Conclusion

Based on positron annihilation measurements for iron and nickel irradiated with hydrogen and helium ions at 423 and 573 K, the following conclusions were obtained. A comparison of long lifetimes showed that the vacancy clustering was more efficient in nickel than in iron. Helium atoms were more effective for microvoid formation than hydrogen atoms. The temperature dependence of microvoid growth was greater after hydrogen-ion irradiation than helium-ion irradiation and it was explained by the instability of hydrogen–vacancy complexes and the stability of helium–vacancy complexes. The comparison of the *S*-parameter ratio and the annealing behavior in nickel between hydrogen and helium-ion irradiation also indicated the difference in the

stability between the hydrogen–vacancy and the helium–vacancy complex.

References

[1] J.B. Conndon, T. Shober, J. Nucl. Mater. 207 (1993) 1.
[2] K. Farrell, Rad. Eff. 53 (1980) 175.
[3] W. Brandt, A. Dupasquier, Positron Solid State Physics, in: Proceedings of the International School of Physics Enrico Fermi, 1983.
[4] M.J. Puska, R.M. Nieminen, Rev. Mod. Phys. 66 (1994) 841.
[5] S. Matsui, J. Phys. Soc. Jpn. 61 (1992) 187.
[6] P. Asoka-Kumar, M. Alatalo, V.J. Ghosh, A.C. Kruseman, B. Nielsen, K.G. Lynn, Phys. Rev. Lett. 77 (1996) 2097.
[7] P.E. Mijnarends, A.C. Kruseman, A. van Veen, H. Sshut, A. Bansil, J. Phys.: Cond. Matter 10 (1998) 10383.
[8] Y. Nagai, M. Hasegawa, Z. Tang, A. Hempel, K. Yubuta, T. Shimamura, Y. Kawazoe, A. Kawai, F. Kano, Phys. Rev. B 61 (2000) 6574.
[9] K.G. Lynn, J.R. MacDonald, R.A. Boie, L.C. Feldman, J.D. Gabbe, M.F. Robbins, E. Bonderup, J. Golovchenko, Phys. Rev. Lett. 38 (1977) 241.
[10] S.I. Golubov, B.N. Singh, H. Trinkaus, J. Nucl. Mater. 276 (2000) 78.
[11] K. Kiuchi, R.B. McLellan, Acta Metall. 31 (1983) 961.
[12] S. Linderoth, A.V. Shishkin, Philos. Mag. A 55 (3) (1987) 291.
[13] J. Völkl, G. Alefeld, Hydrogen in metals (basic properties), Top. Appl. Phys. 28 (1978) 321.
[14] H. Rajainmäki, S. Linderoth, H.E. Hansen, R.M. Nieminen, J Phys. F: Met. Phys. 18 (1988) 1109.
[15] D.J. Reed, Rad. Eff. 31 (1977) 129.
[16] T. Tanabe, H. Hirano, S. Imoto, J. Nucl. Mater. 151 (1987) 38.
[17] T. Yamauchi, S. Yamanaka, M. Miyake, J. Nucl. Mater. 179–181 (1991) 308.